Original Article

Imaging diagnosis analysis and literature review of intrapulmonary solitary fibrous tumor

Ye Liu, Yongkang Nie^

Radiology Diagnosis Department, The First Medical Center of Chinese PLA General Hospital, Beijing, China

Contributions: (I) Conception and design: Y Nie; (II) Administrative support: Y Nie; (III) Provision of study materials or patients: Y Liu; (IV) Collection and assembly of data: Y Liu; (V) Data analysis and interpretation: Y Liu; (VI) Manuscript writing: Both authors; (VII) Final approval of manuscript: Both authors.

Correspondence to: Yongkang Nie, Doctor. Radiology Diagnosis Department, The First Medical Center of Chinese PLA General Hospital, 28 Fuxing Road, Haidian District, Beijing 100853, China. Email: nieyongkang1978@163.com.

Background: Solitary fibrous tumor (SFT) of the chest mainly arises from the pleura, but intrapulmonary SFT is rare. This study aimed to review and discuss the chest multislice computed tomography (MSCT) and magnetic resonance imaging (MRI) findings of intrapulmonary SFT and summarize existing literature on the disease in order to improve clinicians' understanding and diagnosis of this disease.

Methods: The imaging findings and clinical data of 4 surgically and pathologically confirmed intrapulmonary SFT cases were retrospectively analyzed in terms of location, morphology, size, density, border, enhancement level of the lesion, and its relationship with surrounding tissue. These findings were combined with a review of 61 cases reported in the literature to characterize the features of intrapulmonary SFT.

Results: A total of 65 patients with intrapulmonary SFT were reviewed, consisting of 30 females and 35 males. Of these cases, 21 had a lesion in the left lower lobe, more than in any other part of the lungs. The lesions were clear, had a quasicircular boundary, and were distinctly separated from surrounding tissue. Under plain scan, the 4 cases investigated in this study showed lesions of even density, and enhanced scanning revealed geographic enhancement in 2 cases. Of the 65 cases examined, 56 cases were benign, and the remaining 9 cases were borderline or malignant.

Conclusions: The imaging findings of intrapulmonary SFT demonstrated certain features, such as lesions with a clear boundary and even density. Imaging examination is important for the diagnosis and differential diagnosis of this disease.

Keywords: Intrapulmonary solitary fibrous tumor (SFT); chest; multislice computed tomography (MSCT); enhanced scan; chest magnetic resonance imaging (MRI)

Submitted Nov 29, 2022. Accepted for publication Aug 15, 2023. Published online Sep 22, 2023.
doi: 10.21037/qims-22-1328
View this article at: https://dx.doi.org/10.21037/qims-22-1328

^ ORCID: 0000-0002-1556-2263.

Introduction

Solitary fibrous tumor (SFT) is a rare mesenchymal neoplasm, features hyperplasia of spindle cells and small staghorn-like branching blood vessels, and accounts for less than 2% of all soft tissue tumors. It is presently defined by the existence of *NAB2-STAT6* fusion. Most cases are low risk, but approximately 10–30% of SFTs demonstrate features of aggressive behavior, such as localized invasion, recurrence, and distant metastasis (1-6). The 2013 World Health Organization (WHO) classification integrates the former denomination of hemangiopericytoma under the SFT nomenclature; the later 2020 WHO classification avoids the terms typical or malignant, as typical SFT is not necessarily synonymous with benign disease (7,8). Thus far, SFTs have been reported in numerous sites, including peritoneum, parotid gland, paranasal sinuses, orbit, skin, and intracranial areas, a fact which supports a mesenchymal rather than a mesothelial origin. Intrapulmonary SFT is quite rare and mostly limited to a few case reports (9). Intrapulmonary SFT, which is seen on imaging as an intrapulmonary lesion with no correlation to the pleura, is histopathology consistent with the pathological diagnosis of SFT, and the pathological findings do not indicate a primary SFT of the lung. Therefore, SFT originating from the pleura cannot be completely excluded. Computed tomography (CT) is presently the first choice for the clinical examination of SFT. The main treatment is resection through radical surgery, which provides patients with relatively good prognosis. This disease lacks clinical specificity and is therefore commonly misdiagnosed. The information of 4 intrapulmonary SFT cases confirmed by operation and pathology in our hospital (The First Medical Center of Chinese PLA General Hospital) and 61 intrapulmonary SFT cases identified by a Chinese- and English-language literature search of the PubMed database were selected for review. We analyzed and summarized the data of these cases in order to provide a helpful reference for doctors to improve their understanding of the disease and its preoperative diagnosis.

Methods

Clinical data

This study retrospectively analyzed information from 65 patients diagnosed with intrapulmonary SFT, with 4 of these cases being confirmed by operation and pathology at our hospital (*Table 1*) and 61 being identified via a search of the Chinese- and English-language literature of the PubMed database. The group of 65 patients consisted of 30 female and 35 male patients, with a mean age of 58 years (range, 7–83 years) (refer to *Table 2* for information on clinical manifestations). The 4 cases were diagnosed before surgery as benign nodules in 2 cases, neurogenic tumor in 1 case, and lung cancer in 1 case. This study was conducted in accordance with the Declaration of Helsinki (as revised in 2013) and was approved by the ethics committee of The First Medical Center of Chinese PLA General Hospital. Individual consent for this retrospective analysis was waived.

Metastatic risk assessment

Metastatic risk scores were calculated using a 4-variable model reported by Demicco *et al.* in 2017 (1). Patient age was scored as 0 if <55 years and 1 if ≥55 years; tumor size was scored as 0 if <5 cm, 1 if 5 to <10 cm, 2 if 10 to <15 cm, and 3 if ≥15 cm; mitotic activity was scored as 0 if <1 mitotic figure/10 high-power field (HPF), 1 if 1–3 mitotic figures/10 HPF, or 2 if ≥4/10 HPF; and tumor necrosis was scored 0 if <10% and 1 if ≥10%. Total scores were summed, and scores of 0–3 were considered low risk, 4–5 as intermediate risk, and 6–7 as high risk.

Research methods

Three patients received nonenhanced and enhanced 64-slice

Table 1 Features of 4 cases of intrapulmonary SFT

Cases	Sex	Age (years)	Symptoms	Localization	Size (mm)	Density	Enhancement degree	Margin	Risk score
1	Female	42	Asymptomatic	Right lower lobe	15	Even	Map pattern enhancement	Clear	Low risk
2	Male	23	Asymptomatic	Right lower lobe	15	Even	Mild	Clear	Low risk
3	Male	31	Asymptomatic	Right lower lobe	29×23	Even	Mild	Clear	Low risk
4	Male	56	Asymptomatic	Left lower lobe	13	Even	Mild	Clear	Low risk

SFT, solitary fibrous tumor.

Table 2 Features of intrapulmonary SFT cases from the literature

Features	Values
No. of studies (cases)	61
Age (years)	
Mean	58
Range	7–83
Sex	
Male	32
Female	29
Tumor size (mm)	
Mean	63
Range	12–900
Symptoms	
Unknown	31
Asymptomatic	30
Cough	4
Chest pain	4
Chest discomfort	1
Symptomatic hypoglycemia	1
Localization	
Unknown	7
Right lung	3
Left lung	5
Right upper lobe	12
Right middle lobe	3
Right lower lobe	7
Left upper lobe	4
Left lower lobe	20
Treatment	
Surgery	60
Radiofrequency ablation	1
Histology	
Low grade	52
Intermediate or high grade	9

SFT, solitary fibrous tumor.

chest scans preoperatively using a LightSpeed CT (GE HealthCare, Waukesha, USA) and a Brilliance 256 iCT (Philips, Amsterdam, The Netherlands) scanners. Lying in a supine position, the patient was scanned from the apex of the lung to 3 centimeters below the diaphragm, with the whole procedure completed under a breath-hold at the end of inspiration. The scan parameters were as follows: tube voltage, 120 kVp; automatic tube current modulation; and thin layer reconstruction layer thickness, 1.0–1.5 mm. The lung window width and level were 1,600 Hounsfield units (HU) and –600 HU, respectively; the mediastinum window width and level were 400 HU and 40 HU, respectively. The enhanced scan used nonionic contrast medium [70–90 mL of iohexol or iopromide (300 mgI/mL); velocity 3.5 mL/s], and scans for the arterial phase and the venous phase were performed at 25–30 s and 60–65 s, respectively, after injection of the contrast medium.

One patient underwent chest magnetic resonance imaging (MRI) plain and enhanced scanning in a GE HealthCare Signal HDX 3.0T MR scanner with torso coils. Before the procedure, the patient was trained to breathe calmly. The scanning range was from the superior aperture of the thorax to cover the whole diaphragm. The scanning sequences included the following: (I) real time coronal respiratory gating (COR RT) fast spin echo (FSE) T2 [repetition time (TR): 6,000 ms; time to echo (TE): 85 ms]; (II) sagittal single shot FSE (SAG SSFSE; TR: 1,400 ms; TE: 85 ms); (III) axial spoiled gradient echo (AX SPGR) T1 (TR: 200 ms; TE: 2.6 ms); (IV) AX RT IDEAL (Iterative Dixon water-fat separation with Echo Asymmetry and Leastsquares estimation) T2 [TR: 5,000–8,000 ms; TE: 85 ms; echo train length (ETL): 18]; (V) and single-shot AX diffusion-weighted (DW) spin-echo echo planar imaging [SE-EPI; TR: 6,600 ms, TE: 58 ms; fat-suppressed T2-weight imaging (T2WI): TR: 10,000 ms, TE: 74 ms]. Except for the breath-holding scanning of AX SPGR T1, all the other sequences used free breathing and respiratory gating techniques.

Subsequently, dynamic-enhanced scanning was performed in the cross-sectional, sagittal and coronal planes after injection of a gadolinium-diethylenetriamine-pentaacetic acid (Gd-DTPA) contrast agent bolus in a vein of the elbow at a flow rate of 2.0 mL/s.

Results

Imaging findings

Of the 4 patients with intrapulmonary SFT, 3 tumors

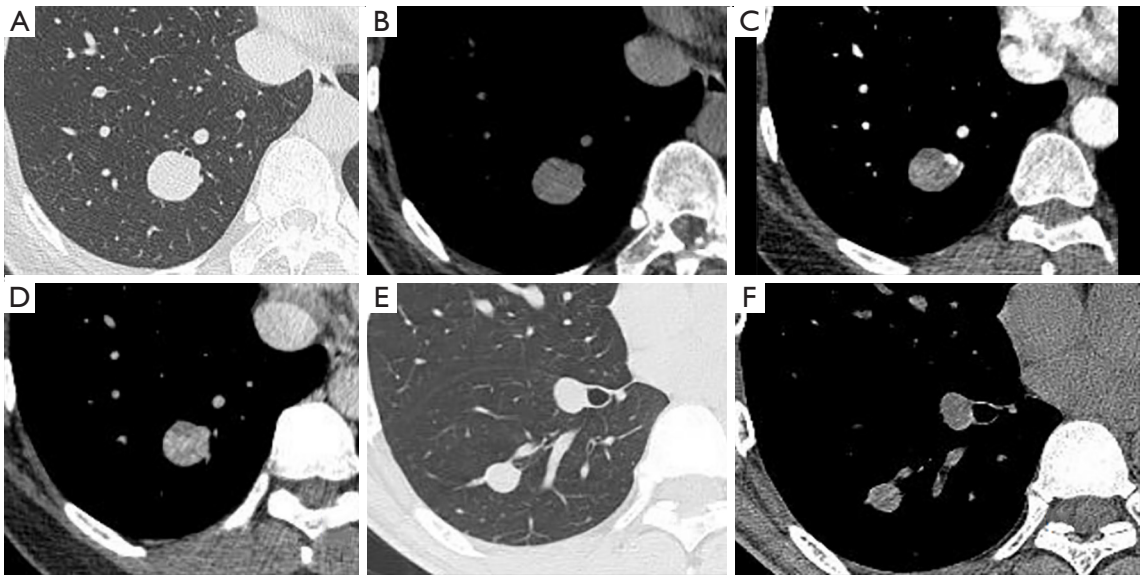

Figure 1 Images from Cases 1 (A-D: chest CT scan) and 2 (E,F: chest CT scan). Case 1: A 42-year-old female with nodules in right lower lobe identified in physical examination. (A-D) Chest CT nonenhanced and enhanced scans. (A) Lung window: quasicircular nodules, approximately 19 mm in diameter, observed in the posterior basal segment of the right lower lobe. (B) Mediastinum window: nodules of even density, with a CT attenuation value of about 26 HU. (C,D) Enhanced scan: mild enhancement during the arterial phase, with a CT attenuation value of about 37 HU; uneven enhancement during the venous phase, with a CT attenuation value of about 4–133 HU and a blood vessel running along the margin of the lesion. Case 2: A 23-year-old male with nodules in the right lower lobe identified in physical examination. (E,F) Chest CT scans. (E) Lung window: quasicircular nodules, approximately 15 mm in diameter, observed in the dorsal segment of the right lower lobe. (F) Mediastinum window: nodules of even density, and a CT attenuation value about 27 HU. CT, computed tomography; HU, Hounsfield units.

were located in the right lower lobe and 1 in the left lower lobe. One patient presented with a broad-based tumor growing close to the pleura. In terms of size and the morphology and density of the lesion, 4 patients with SFT showed quasicircular or oval lesions, with the largest lesion being 29 mm × 23 mm in size; 3 cases showed soft tissue shadows of even density but no calcification; 2 cases showed no obvious enhancement in the arterial phase; and 1 case showed geographic enhancement. One case showed a long T1, slightly long T2 signal, and slightly high diffusion-weighted imaging (DWI) signal intensity, without significant signal diminution during the positive and negative phases; dynamic-enhanced scanning revealed uneven continuous enhancement and a fat pad between the tumor and the adjacent pleura. In terms of peripheral changes, 4 cases had lesions with a clear boundary, and 1 case had a tumor growing adjacent to the visceral pleura. In all cases, the tumor did not invade the visceral pleura, and an obvious, normal, and uninvolved lung parenchyma edge was observed to be separating the tumor mass from the surface of the pleura covering it (*Figures 1*,*2*).

Pathologic results

In the 4 cases from our hospital, the solitary nodules were all located in the lung parenchyma. In 1 case, the nodule was quasicircular, had a distinct border, and showed no obvious cytologic atypia. Images indicated a mitotic rate at 2/10 HPF. The tumor cells were fusiform, and the tumor stroma contained rich collagen and observable staghorn-like blood vessels. No necrosis was found, and the lesion was lobulated focally and accompanied by alveolar epithelial lining. All the features indicated the benignity of the tumor, and when combined with the immunophenotype, pointed to SFT. Immunohistochemical (IHC) staining of the tumor cells indicated the following: vimentin (+), Bcl-2 (+), Ki-67 (+<10%), CD99 (–), CD34 (–), vessel disease (+), and S-100 (–). In the other 3 cases, the lesions were quasicircular or oval, with a clear border but no obvious cytologic atypia. The mitotic rate was

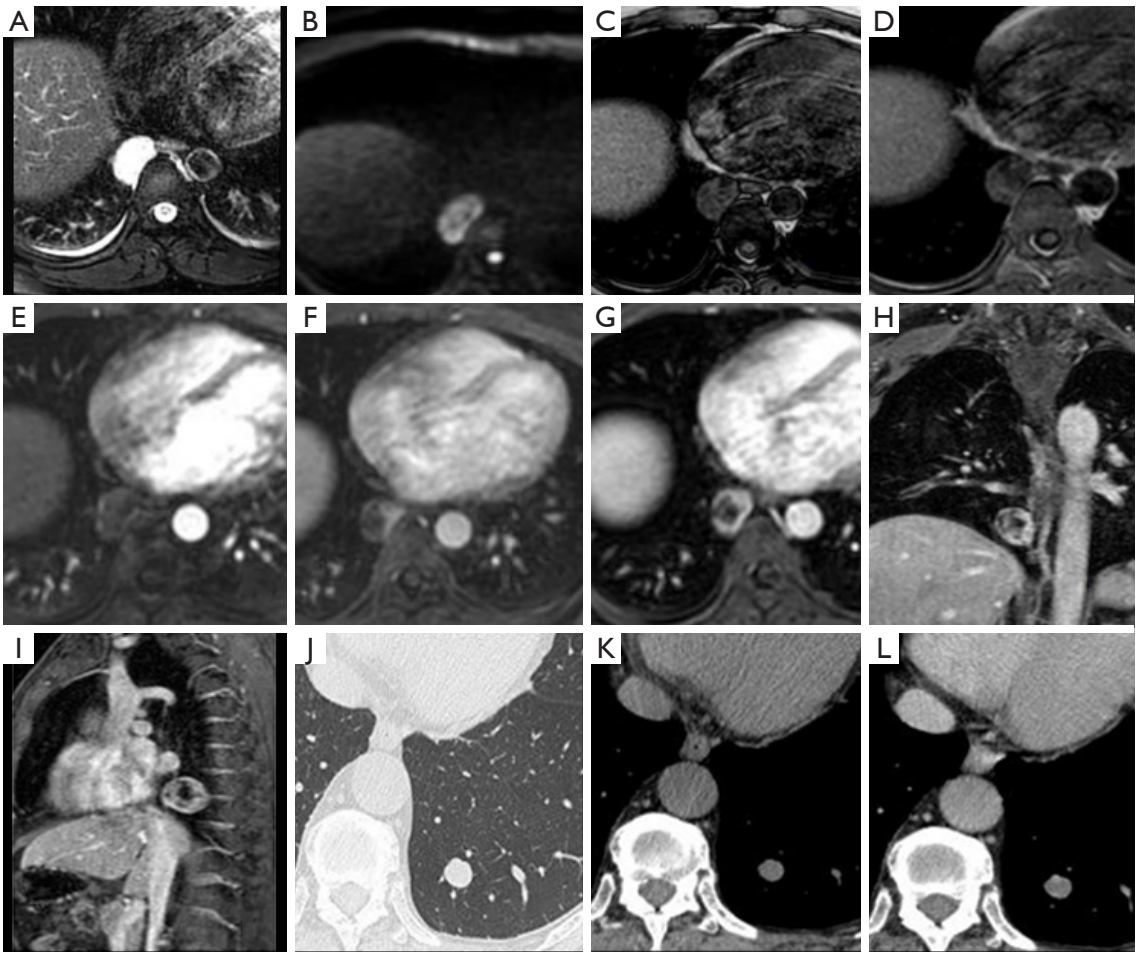

Figure 2 Images from Cases 3 (A-I: chest MRI scan) and 4 (J-L: chest CT scan). Case 3: A 31-year-old male with nodules beside the posterior mediastinum discovered in physical examination. (A-I) Chest MRI nonenhanced and enhanced scans. (A) Axial T2WI: a quasicircular smooth-edged shadow about 29 mm × 17 mm × 23 mm beside the posterior mediastinum of the right lower lobe and long T1 and T2 signals. (B) DWI: hyperintensity. (C,D) No signal diminution in positive or negative phase signals. (E-G) Enhanced scanning: dynamic-enhanced scans showing continuous uneven enhancement. (H) Coronary scan and (I) sagittal scan: lesions distinctly separated from surrounding tissues. Case 4: A 56-year-old male with nodules in left lower lobe identified in physical examination. (J-L) Chest CT nonenhanced and enhanced scans. (J) Lung window: quasicircular nodules, approximately 13 mm in diameter, observed in the posterior basal segment of the left lower lobe. (K) Mediastinum window: nodules of even density, with a CT attenuation value of about 28 HU. (L) Enhanced scan: mild enhancement during the arterial-venous phase, with a blood vessel running along the margin of the lesion. MRI, magnetic resonance imaging; CT, computed tomography; T2WI, T2-weight imaging; DWI, diffusion-weighted imaging; HU, Hounsfield units.

2/10 HPF, substantial stromal collagen accumulation was evident, staghorn-like blood vessels were observable in the stroma, and no necrosis was found. IHC staining results indicated the following: SMA (smooth muscle antigen) (–), S-100 (–), h-caldesmon (partially weak+), CD34 (+), Bcl-2 (+), STAT6 (signal transducer and activator of transcription 6) (nuclear+), Ki-67 (+8%), and cytokeratin (–) (*Figure 3*). All 4 cases were low risk (see *Table 1*).

Discussion

SFT originates from a rare mesenchymal tumor differentiating from dendritic mesenchymal cells expressing the CD34 antigen. Its incidence rate is 1.4 per million

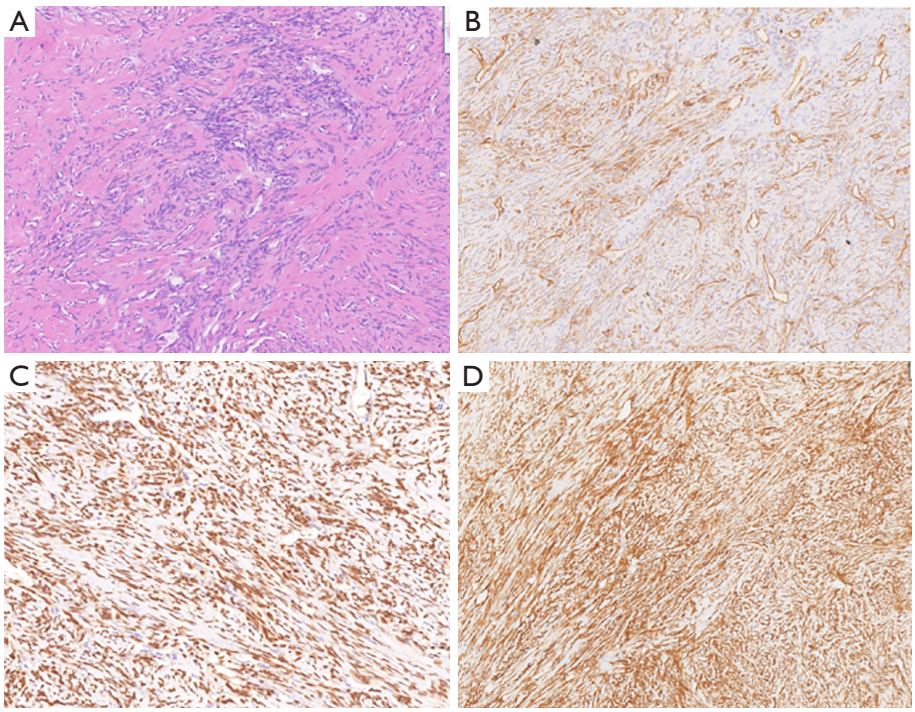

Figure 3 Pathology results. (A) (HE ×100) Spindle cell tumor with a clear border, no obvious cytologic atypia, conspicuous stromal collagen accumulation, staghorn-like blood vessels visible in the stroma, and no necrosis, indicating SFT. IHC test results (×100): (B) STAT6 (nuclear+), (C) CD34 (+), and (D) Bcl-2 (+). HE, hematoxylin and eosin; SFT, solitary fibrous tumor; IHC, immunohistochemical.

people, with 13–37% of cases being malignant (10). The tumor mainly consists of a large number of spindle cells, which contain abundant mature blood vessels and mature fibrillar collagen (10,11). Spindle cells are widely distributed in the connective tissue of human body, so SFT can occur in any part of the human body, most often in the chest. Typically, SFT first arises in the pleura and can grow along the mediastinal space. However, reports of extrapleural SFTs have gradually increased in number in recent years, with other sites including the peritoneum, kidney, pancreas, thyroid gland, liver, gall bladder, head and face, mediastinum, breast, and the lung (12-17). There have also been sporadic reports of SFT in the lung parenchyma (18-29). According to the literature, intrapulmonary SFT can occur at all ages but tends to affect young adults and older adults, with most malignant cases occurring in those 50 to 70 years of age, with no sex-specific predominance (1,3,4,7,30-33). Generally, the literature indicates that SFT most often occurs in the left lower lobe, without specific clinical manifestations at onset. As the tumor grows gradually in size and compresses surrounding lung tissue and bronchi, patients experience chest tightness, shortness of breath, dyspnea, and other secondary symptoms, as well as paraneoplastic syndromes (PNS), including Doege-Potter syndrome (recurrent hypoglycemia) and Pierre-Marie-Bamberger syndrome (hypertrophic pulmonary osteoarthropathy, long bone periostitis, and arthritis accompanied by clubbed fingers). These syndromes can be relieved after complete resection of the tumor (34-36). For the 4 cases in this study, the tumors were all less than 30 mm in diameter and triggered no symptoms.

As far back as 1942, Stout and Murray described the intrapulmonary location of these tumors, but it seems that in these early descriptions, the tumors originated from the visceral pleura with a "growth pattern" (37). In this study, the imaging findings of 1 case showed that the disease was closely related to the visceral pleura, and the postoperative pathological findings indicated an intrapulmonary origin. Under most circumstances, intrapulmonary SFTs grow slowly, are asymptomatic at onset and during the course of progression, and are often found during routine physical examination. The intrapulmonary origination of SFT might be attributable to (I) the direct continuity between the mesenchyme and subpleural intralobular septa, (II)

parenchymal lung fibroblasts, or (III) indentation of visceral pleura. This topic stems from two assumptions (26). First, the direct continuity of the subpleural mesenchyme and interlobular septa or indentation of visceral pleura can cause pulmonary SFT. Second, these tumors originate from the facultative fibroblast elements in the subcutaneous area of the normal pulmonary parenchyma. It was reported that these elements have ultrastructural and IHC characteristics similar to those of subpleural connective tissue (38). All 4 cases in this study occurred in the lungs, were found on routine physical examination, and demonstrated no clinical or radiological characteristics, which hindered preoperative diagnosis. Excisional biopsy and histopathological examination are usually required (39). Fine needle aspiration or bronchoscopic biopsy is often inadequate for providing reliable therapeutic guidance (40).

Imaging findings of intrapulmonary SFT is usually benign and with a low risk of potential tumor (41). Its imaging features include slow growth, clear border, possible lobulation, absence of spicule sign and satellite lesions, uniform density in most cases, and calcification (about 7–26%) and necrosis in a few cases. The presence of calcification has no obvious correlation with low risk or high risk of malignancy in tumors, but may be related to necrosis (42). Alghamdi *et al.* reported calcification (in 1 case) (36). The 4 cases in this study did not show specific calcification, and since the tumors were small, there was no necrosis. Some cases with lesion located in the posterior thoracic cavity can also have manifestations similar to those of neurogenic tumors, which is why 1 case in this study was diagnosed as neurogenic tumor before operation. Under enhanced scanning, SFT showed enhancement in a variety of ways. Low-risk SFTs are well supplied, mainly by the internal thoracic artery and bronchial artery. High-risk SFTs have an unclear boundary, uneven density, rough edge, and signs of invasion of the surrounding tissue. The possibility of high-risk SFTs should be considered if the mass grows rapidly, is large (>10 cm), and invades adjacent tissue or has distant metastasis. Under enhanced scanning, most of the SFT cases showed moderate-to-severe uneven enhancement, and the enhancement level was about 45–100 HU (43). Wu *et al.* reported a case of SFT being diagnosed as central lung cancer preoperatively, where the right main bronchus and the middle segmental bronchus were obstructed, with secondary atelectasis of all lobes; the mass showed relatively even density under plain scan but uneven enhancement under scanning with contrast (31). Two cases in this study presented with no obvious enhancement in the arterial phase, and mild enhancement in the delayed phase; in contrast-enhanced scanning, obviously enhanced linear and strip vascular shadows were seen in part of the lesion in on case, and uneven continuous enhancement was seen in the other case. The CT findings of SFT are related to the size of the lesion. A small lesion has even density and clear boundary, with few accompanying signs. A comparatively large lesion has uneven density, an unclear boundary, and many accompanying signs. As the tumor grows bigger, the probability of the sign of pleural effusion also grows. The 4 cases of this study all showed pathological features of benign tumor, and imaging findings indicated no malignant signs.

Pathological findings of intrapulmonary SFT

There is no significant difference in the clinical, histopathological, or IHC features between intrapulmonary SFT and pleural SFT (30). SFT is generally a quasicircular or lobulated solid mass with a complete capsule or fibrous pseudocapsule, having a well-defined border. Observed under a microscope, the tumor tissue is rich in collagenous fibers and spindle tumor cells, which are mixed in different proportions to form dense and sparse areas of cells, with the spindle cells being arranged without a fixed pattern; these are the pathological features of SFT. A large number of collagenous fibers can be seen in the tumor stroma. Some parts demonstrate mucoid or cystic changes, while some parts contain abundant blood vessels, dilated vascular lumens, hyaline degeneration of vascular walls, and focal hemangiopericytoma-like structures. The positive markers on IHC tests mainly include CD34, vimentin, CD99, and Bcl-2. The majority of SFT cases are CD34 positive, which is specific for the diagnosis of SFT. When the expression of CD34 is negative, the positive expression of Bcl-2 can still be used to diagnose SFT (44). In this study, 1 of the 4 patients showed CD34 (–). Negative markers mainly include S-100, CK, Desmin, SMA, and EMA (epithelial membrane antigen). A large number of studies have shown that STAT6 is the most sensitive and specific marker for diagnosing SFT, which is consistent with a study showing a 96% positive rate of STAT6 expression in all SFT cases examined (45). In our study, we found that the positive rate of vimentin among confirmed SFT cases was 100%. Therefore, the above markers can be used in combination to diagnose SFT. In addition, except with respect to the Ki-67 index, low-risk and high-risk SFTs showed no difference in the IHC test results. Therefore, CT scanning, especially

the high-resolution multislice mode, is a reliable method for differentiating high-risk and low-risk SFTs. As a general rule, it is suggested that (I) the lesion be completely resected and that (II) all patients be monitored with long-term follow-up (46).

Intrapulmonary SFT is mainly a low-risk tumor, and typical imaging findings are benign. High-risk intrapulmonary SFT is also rare tumor and need not essential to differentiate from intrapulmonary malignant SFTs; instead, it should be differentiated from other intrapulmonary malignant tumors. Intrapulmonary SFT generally needs to be differentiated from the following diseases, among others: benign intrapulmonary tumors, such as pulmonary sclerosing pneumocytoma (PSP), hamartoma, and granulomatous nodules; neurogenic tumors, more often than not found in the posterior mediastinum; intrapulmonary single metastatic tumor; peripheral lung cancer; Castleman disease; and sarcomatoid carcinoma. Without specific imaging findings, intrapulmonary SFT is easily misdiagnosed as another disease, and preoperative diagnosis and differential diagnosis mainly relies on pathological and IHC test results obtained from tumor biopsy via needle puncture and aspiration.

Intrapulmonary SFT is mainly treated by complete surgical resection. Even when the disease is pathologically diagnosed as low risk, SFT still has the potential for malignancy, and the possibility of relapse or deterioration after complete resection cannot be ruled out. Inoue *et al.* reported a local relapse of SFT 2 years after nonanatomic wedge resection performed on the left upper lobe and emphasized the importance of long-term postoperative follow-up for benign tumors (47). Wu *et al.* reported metastasis to the diaphragm and abdominal cavity 5 months after operation in 1 high-risk SFT case (31). As for the 4 cases treated by our hospital, 1 case showed no abnormalities in chest CT scans during the 24-month follow-up, while the other 3 cases were not followed up. The study had several limitations related to its retrospective nature and small sample size.

Conclusions

Since intrapulmonary SFT is clinically nonspecific, the discovery of lesions mainly depends on imaging. Multislice CT has high spatial and temporal resolution, which can not only display the small and microstructures of the lesion but can also enable the observation of the periphery and supplying blood vessels of the lesion from various angles via the multiplanar reconstruction technique. Although intrapulmonary SFTs are often low risk, existing data demonstrate that these tumors necessitate the extension of close clinical follow-up (48).

Acknowledgments

Funding: None.

Footnote

Conflicts of Interest: Both authors have completed the ICMJE uniform disclosure form (available at https://qims.amegroups.com/article/view/10.21037/qims-22-1328/coif). The authors have no conflicts of interest to declare.

Ethical Statement: The authors are accountable for all aspects of the work in ensuring that questions related to the accuracy or integrity of any part of the work are appropriately investigated and resolved. The study was conducted in accordance with the Declaration of Helsinki (as revised in 2013) and was approved by the ethics committee of The First Medical Center of Chinese PLA General Hospital. Individual consent for this retrospective analysis was waived.

References

1. Demicco EG, Wagner MJ, Maki RG, Gupta V, Iofin I, Lazar AJ, Wang WL. Risk assessment in solitary fibrous tumors: validation and refinement of a risk stratification model. Mod Pathol 2017;30:1433-42.
2. Ronchi A, Cozzolino I, Zito Marino F, Accardo M, Montella M, Panarese I, Roccuzzo G, Toni G, Franco R, De Chiara A. Extrapleural solitary fibrous tumor: A distinct entity from pleural solitary fibrous tumor. An update on clinical, molecular and diagnostic features. Ann Diagn Pathol 2018;34:142-50.

3. Demicco EG, Park MS, Araujo DM, Fox PS, Bassett RL, Pollock RE, Lazar AJ, Wang WL. Solitary fibrous tumor: a clinicopathological study of 110 cases and proposed risk assessment model. Mod Pathol 2012;25:1298-306.
4. Gholami S, Cassidy MR, Kirane A, Kuk D, Zanchelli B, Antonescu CR, Singer S, Brennan M. Size and Location are the Most Important Risk Factors for Malignant Behavior in Resected Solitary Fibrous Tumors. Ann Surg Oncol 2017;24:3865-71.
5. Pasquali S, Gronchi A, Strauss D, Bonvalot S, Jeys L, Stacchiotti S, Hayes A, Honore C, Collini P, Renne SL, Alexander N, Grimer RJ, Callegaro D, Sumathi VP, Gourevitch D, Desai A. Resectable extra-pleural and extra-meningeal solitary fibrous tumours: A multi-centre prognostic study. Eur J Surg Oncol 2016;42:1064-70.
6. Salas S, Resseguier N, Blay JY, Le Cesne A, Italiano A, Chevreau C, et al. Prediction of local and metastatic recurrence in solitary fibrous tumor: construction of a risk calculator in a multicenter cohort from the French Sarcoma Group (FSG) database. Ann Oncol 2017;28:1979-87.
7. Fletcher CD. The evolving classification of soft tissue tumours - an update based on the new 2013 WHO classification. Histopathology 2014;64:2-11.
8. Kallen ME, Hornick JL. The 2020 WHO Classification: What's New in Soft Tissue Tumor Pathology? Am J Surg Pathol 2021;45:e1-23.
9. Zhang K, Liu HJ, Cheng ZB, Deng M, Luo J, Qi X. Solitary fibrous tumor: a 10-year retrospective analysis with several rare cases. Chin Med J (Engl) 2020;134:1006-8.
10. Thorgeirsson T, Isaksson HJ, Hardardottir H, Alfredsson H, Gudbjartsson T. Solitary fibrous tumors of the pleura: an estimation of population incidence. Chest 2010;137:1005-6.
11. Ardissone F. Thoracic malignant solitary fibrous tumors: Prognostic factors and long-term survival. J Thorac Dis 2011;3:84-5.
12. Silvanto A, Karanjia ND, Bagwan IN. Primary hepatic solitary fibrous tumor with histologically benign and malignant areas. Hepatobiliary Pancreat Dis Int 2015;14:665-8.
13. Feasel P, Al-Ibraheemi A, Fritchie K, Zreik RT, Wang WL, Demicco E, Saeb-Lima M, Goldblum JR, Rubin BP, McKenney JK, Ko JS, Billings SD. Superficial Solitary Fibrous Tumor: A Series of 26 Cases. Am J Surg Pathol 2018;42:778-85.
14. Thompson LDR, Wei C, Rooper LM, Lau SK. Thyroid Gland Solitary Fibrous Tumor: Report of 3 Cases and a Comprehensive Review of the Literature. Head Neck Pathol 2019;13:597-605.
15. Bauer JL, Miklos AZ, Thompson LD. Parotid gland solitary fibrous tumor: a case report and clinicopathologic review of 22 cases from the literature. Head Neck Pathol 2012;6:21-31.
16. O'Regan EM, Vanguri V, Allen CM, Eversole LR, Wright JM, Woo SB. Solitary fibrous tumor of the oral cavity: clinicopathologic and immunohistochemical study of 21 cases. Head Neck Pathol 2009;3:106-15.
17. Insabato L, Siano M, Somma A, Gentile R, Santangelo M, Pettinato G. Extrapleural solitary fibrous tumor: a clinicopathologic study of 19 cases. Int J Surg Pathol 2009;17:250-4.
18. England DM, Hochholzer L, McCarthy MJ. Localized benign and malignant fibrous tumors of the pleura. A clinicopathologic review of 223 cases. Am J Surg Pathol 1989;13:640-58.
19. van de Rijn M, Lombard CM, Rouse RV. Expression of CD34 by solitary fibrous tumors of the pleura, mediastinum, and lung. Am J Surg Pathol 1994;18:814-20.
20. Schirosi L, Lantuejoul S, Cavazza A, Murer B, Yves Brichon P, Migaldi M, Sartori G, Sgambato A, Rossi G. Pleuro-pulmonary solitary fibrous tumors: a clinicopathologic, immunohistochemical, and molecular study of 88 cases confirming the prognostic value of de Perrot staging system and p53 expression, and evaluating the role of c-kit, BRAF, PDGFRs (alpha/beta), c-met, and EGFR. Am J Surg Pathol 2008;32:1627-42.
21. Yousem SA, Flynn SD. Intrapulmonary localized fibrous tumor. Intraparenchymal so-called localized fibrous mesothelioma. Am J Clin Pathol 1988;89:365-9.
22. Aufiero TX, McGary SA, Campbell DB, Phillips PP. Intrapulmonary benign fibrous tumor of the pleura. J Thorac Cardiovasc Surg 1995;110:549-51.
23. Baliga M, Flowers R, Heard K, Siddiqi A, Akhtar I. Solitary fibrous tumor of the lung: a case report with a study of the aspiration biopsy, histopathology, immunohistochemistry, and autopsy findings. Diagn Cytopathol 2007;35:239-44.
24. Caruso RA, LaSpada F, Gaeta M, Minutoli I, Inferrera C. Report of an intrapulmonary solitary fibrous tumor: fine-needle aspiration cytologic findings, clinicopathological, and immunohistochemical features. Diagn Cytopathol 1996;14:64-7.
25. Kanamori Y, Hashizume K, Sugiyama M, Motoi T, Fukayama M, Ida K, Igarashi T. Intrapulmonary solitary fibrous tumor in an eight-year-old male. Pediatr Pulmonol

2005;40:261-4.
26. Kouki HS, Koletsis EN, Zolota V, Prokakis C, Apostolakis E, Dougenis D. Solitary fibrous tumor of the lung. Gen Thorac Cardiovasc Surg 2008;56:249-51.
27. Patsios D, Hwang DM, Chung TB. Intraparenchymal solitary fibrous tumor of the lung: an uncommon cause of a pulmonary nodule. J Thorac Imaging 2006;21:50-3.
28. Sagawa M, Ueda Y, Matsubara F, Sakuma H, Yoshimitsu Y, Aikawa H, Usuda K, Minato H, Sakuma T. Intrapulmonary solitary fibrous tumor diagnosed by immunohistochemical and genetic approaches: report of a case. Surg Today 2007;37:423-5.
29. Sakurai H, Tanaka W, Kaji M, Yamazaki K, Suemasu K. Intrapulmonary localized fibrous tumor of the lung: a very unusual presentation. Ann Thorac Surg 2008;86:1360-2.
30. Rao N, Colby TV, Falconieri G, Cohen H, Moran CA, Suster S. Intrapulmonary solitary fibrous tumors: clinicopathologic and immunohistochemical study of 24 cases. Am J Surg Pathol 2013;37:155-66.
31. Wu B, Chen L, Wang N, Wu L, Yu D, Dou L. One case of lung malignant solitary fibroma and literature review. Chinese Journal of Laboratory Diagnosis 2013;17:1151-2.
32. Wu C, Liu C, Shi Q, Zhou H, Zhang R, Lu Z. Lung solitary fibrous tumor with sarcomatous transformation: report of a case and review of literature. Journal of Diagnostics Concepts & Practice 2010;9:572-5.
33. Liu C, Wang J, Mao Min, Lin M. Isolated fibrous tumor of the lung: a case report. Chinese Journal of Diagnostic Pathology 2010;17:320.
34. Chang ED, Lee EH, Won YS, Kim JM, Suh KS, Kim BK. Malignant solitary fibrous tumor of the pleura causing recurrent hypoglycemia; immunohistochemical stain of insulin-like growth factor i receptor in three cases. J Korean Med Sci 2001;16:220-4.
35. Boyer-Duck E, Dajer-Fadel WL, Hernández-Arenas LÁ, Macías-Morales MP, Rodríguez-Gómez A, Romo-Aguirre C. Pierre-Marie-Bamberger syndrome and solitary fibrous tumor: a rare association. Asian Cardiovasc Thorac Ann 2018;26:154-7.
36. Alghamdi ZM, Othman SA, Al-Yousef MJ, AlFadel BZ. Intrapulmonary location of benign solitary fibrous tumor. Ann Thorac Med 2020;15:98-101.
37. Stout AP, Murray MR. Hemangiopericytoma: a vascular tumor featuring Zimmerman's pericytes. Ann Surg 1942;116:26-33.
38. Carretta A, Bandiera A, Melloni G, Ciriaco P, Arrigoni G, Rizzo N, Negri G, Zannini P. Solitary fibrous tumors of the pleura: Immunohistochemical analysis and evaluation of prognostic factors after surgical treatment. J Surg Oncol 2006;94:40-4.
39. Robinson LA. Solitary fibrous tumor of the pleura. Cancer Control 2006;13:264-9.
40. Cardillo G, Facciolo F, Cavazzana AO, Capece G, Gasparri R, Martelli M. Localized (solitary) fibrous tumors of the pleura: an analysis of 55 patients. Ann Thorac Surg 2000;70:1808-12.
41. Shinya T, Masaoka Y, Sando M, Tanabe S, Okamoto S, Ihara H, Tanaka T, Otani S, Hiraki T, Kanazawa S. Imaging an intrapulmonary solitary fibrous tumor with CT and F-18 FDG PET/CT. Radiol Case Rep 2019;14:755-8.
42. Zhang Y, Ba Z, Zhao S. MSCT Findings of Solitary Fibrous Tumors of the Chest. Chinese Journal of Medical Imaging 2010;18:443-7.
43. Sun Yi, Xie L, Hu C, Xv K. The MSCT features of thoracic solitary fibrous tumor. Radiologic Practice 2015;30:236-9.
44. Zhu Y, Du K, Ye X, Song D, Long D. Solitary fibrous tumors of pleura and lung: report of twelve cases. J Thorac Dis 2013;5:310-3.
45. Yuzawa S, Nishihara H, Wang L, Tsuda M, Kimura T, Tanino M, Tanaka S. Analysis of NAB2-STAT6 Gene Fusion in 17 Cases of Meningeal Solitary Fibrous Tumor/Hemangiopericytoma: Review of the Literature. Am J Surg Pathol 2016;40:1031-40.
46. Zhang J, Liu J, Zhang Z, Tian B. Solitary Fibrous Tumors of the Chest: An Analysis of Fifty Patients. Front Oncol 2021;11:697156.
47. Inoue T, Owada Y, Watanabe Y, Muto S, Okabe N, Yonechi A, Kanno R, Suzuki H. Recurrent Intrapulmonary Solitary Fibrous Tumor With Malignant Transformation. Ann Thorac Surg 2016;102:e43-5.
48. Badawy M, Nada A, Crim J, Kabeel K, Layfield L, Shaaban A, Elsayes KM, Gaballah AH. Solitary fibrous tumors: Clinical and imaging features from head to toe. Eur J Radiol 2022;146:110053.

Cite this article as: Liu Y, Nie Y. Imaging diagnosis analysis and literature review of intrapulmonary solitary fibrous tumor. Quant Imaging Med Surg 2023;13(12):8303-8312. doi: 10.21037/qims-22-1328

